FACTA UNIVERSITATIS
Series: **Electronics and Energetics** Vol. 31, N^o 3, September 2018, pp. 425-445
https://doi.org/10.2298/FUEE1803425D

ELECTRIC FIELD MODELING AND ANALYSIS OF EHV POWER LINE USING IMPROVED CALCULATION METHOD

Rabah Djekidel, Sid Ahmed Bessedik, Abdechafik Hadjadj

Laboratory for Analysis and Control of Energy Systems and Electrical Systems
LACoSERE, Laghouat University (03000), Algeria

Abstract. *This paper aims is devoted to modeling and simulation of electric field created by EHV power transmission line of 275 kV using an efficient hybrid methodology, the charge simulation method (CSM) with the Simplex Simulated Annealing (SIMPSA) algorithm in order to find the optimal position and number of fictitious charges used in CSM for an accurate calculation. Various factors that affect the electric field intensity were analyzed; it is found that the influence of the conductor sagging is clearly remarked, the maximum electric field strength at 1 m above the ground level recorded at mid-span point of the power line is 3.09 kV/m, in the proximity of the pylon, the maximum value is significantly reduced to 1.28 kV/m. The configuration type of the transmission line (single or double circuit) and the arrangements of phase conductors on double circuit pylons have a significant effect on the levels of electric field around the transmission line. For a single circuit, the triangular configuration provides the lowest maximum value of electric field. For a double circuit, the inverse phase arrangement (abc-cba) or low-reactance phasing produces the lowest maximum value of electric field. The resulting maximum electric field levels were found below the exposure values set by the ICNIRP and IRPA standards for both occupational and general public. The simulation results of electric field are compared with those obtained from the COMSOL 4.3b Multiphysics software, a fairly good agreement is found.*

Key words: *Catenary Geometry, Charge Simulation Method (CSM), Electric Field, EHV Power Line, Simplex Simulated Annealing (SIMPSA)*

Received October 7, 2017; received in revised form March 19, 2018
Corresponding author: Djekidel Rabah
Laboratory for Analysis and Control of Energy Systems and Electrical Systems LACoSERE, Laghouat University (03000), Algeria
(E-mail: rabah03dz@live.fr)

1. INTRODUCTION

Over the years, electricity has improved the conditions of human life; it plays a key role in responding to basic human needs. However, despite all its advantages, electricity has many negative effects on human health identified. As energy needs increase with the rapid growth of the human population, leading to adoption of electric transport systems with very high voltage levels and accelerated the creation of new transmission power lines using single circuit or double circuit near residential areas. The electric and magnetic fields at extremely low frequencies generated by the lines of the transmission network have assumed great importance in recent years, because of growing concern about the potential effects of these fields on human health and the environment. Exposures to these generated fields induce a current inside human bodies that interferes with those of the body and can, if sufficiently intense, cause harmful biological effects with important implications for human health.

In the last years, several publications have been made for the calculation and measurement of very low frequency electric and magnetic fields (ELF) created by power transmission lines [1-5], based on the results and recommendations reported by these research studies. A number of national and international standards have been established, to define the limits for occupational and public exposure of electric and magnetic fields at very low frequency [6-8]. In parallel, a wide variety of software using different numerical techniques have been developed for modeling and simulation of electric and magnetic fields in both 2D and 3D analysis.

The international organizations responsible for providing guidance and advice on the health hazards of non-ionizing radiation exposure officially recognized by the World Health Organization (WHO) are the International Commission against Non-Ionizing Radiation (ICNIRP) and the International Radiation Protection Association (IRPA), usually at a frequency of 50 Hz, these organizations recommend an exposure limit (24 hours), for the general public are of the order of 5 kV/m for the electric field and 100 µT for the magnetic field, as regards the occupational exposure medium, these recommendations are 10 kV/m and 500 µT, respectively [6-8].

Therefore, it is very important to assess the levels of electric and magnetic fields generated by these very-high-voltage transmission lines, in order to protect public health, environmental and electrical equipments [9,10].

In view of the above, the purpose of this paper is to analyze the electric field levels generated by the High Voltage transmission lines (HVTL) in a steady state condition, using a novel modeling approach that combines charge simulation method (CSM) with Simplex Simulated Annealing (SIMPSA).

The charge simulation method, due to its favorable characteristics, such as simplicity and ease of programming, the execution speed, has been very commonly used successfully in many studies to solve a variety of analysis problems of the electric field in high voltage electrical insulation systems [11-20]. To improve the performance of this technique, aiming to increase the calculation accuracy, it seems advisable to use one of the optimization techniques as the Simplex Simulated Annealing (SIMPSA) algorithm in combination with this method in order to determine the optimal number and position of simulation charges. This algorithm shows good robustness and accuracy in arriving at the global optimization of difficult non-convex highly unconstrained and constrained functions; it combines the downhill simplex method (DHS) with Simulated Annealing algorithm (SA) [21,22]. It

should be noted that this calculation takes into account the effects of the catenary line, where the conductor sag depends on the individual characteristics of the electrical line and environmental conditions, this effect is rarely considered in the literature, because most often it is assumed negligible. Usually, they use in the calculation method the notion of the average height of the electrical line. The simulation results will be compared with those obtained using COMSOL Multiphysics 4.3b based on the Finite Element Method.

2. Model of Overhead Power Lines

The conductors of an overhead power line are not at all points at the same height along the span of this line (longitudinal axis). In fact, they regularly describe a catenary, where the sag depends on the individual characteristics of the line and environmental conditions. Fig. 1 depicts the basic catenary geometry for a single conductor line [18,23,24].

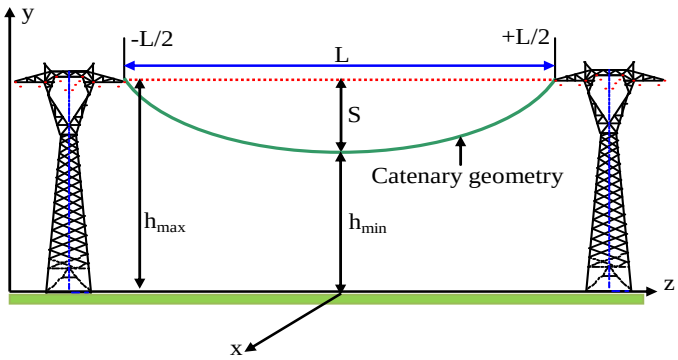

Fig. 1 The basic catenary geometry for a single-conductor line

The equation of the catenary shape of conductor placed in the (yz) plane is given by [25].

$$y(z) = h_{min} + 2\times\alpha\times\sinh^2\left(\frac{z}{2\times\alpha}\right) \tag{1}$$

Where z is the longitudinal position of the conductor about z axis, for a symmetrical line, you normally choose z = 0 at the mid-span; α is the solution of the transcendental equation, with.

$$\frac{S}{2\times\alpha} = \sinh^2\left(\frac{L}{4\times\alpha}\right) \tag{2}$$

To calculate the height of the electrical line along z axis in a span length, the following equation can be used [25].

$$y(z) = h_{\min} + \left(4 \times \frac{S}{L^2} \times z^2 \right) \tag{2}$$

Some researchers, in the electric field calculation in the vicinity of power lines assumes that the conductors are horizontal of infinite length, parallel to a flat ground and parallel with each other, and the sagging due to the weight of conductors is neglected, taking into account an average height between the maximum height and the height minimum of the power line [18]. The average height h_{ave} is given by the following expression.

$$h_{ave} = h_{\max} - \left(\frac{2}{3} \right) \times S \tag{3}$$

Where $h_{\min}$ is the minimum height of the line; $h_{\max}$ is the maximum height; S is the sag of the conductor; L is the length of the power line in one span.

3. CHARGE SIMULATION METHOD (CSM)

The basic principle of this method is very simple. If several discrete charges of any type are present in a region, the electrostatic potential at any point can be found by the superposition of the potentials resulting from the individual charges as long as this point, this potential can be given as follows [11-13].

$$V_i = \sum_{j=1}^{n} P_{ij} \times Q_j \tag{4}$$

Where n is the number of fictitious charges and Pij called the potential coefficient, means the potential at point i caused by a unit charge of Qj.

Once the types of simulation charges and their positions are defined, the simulation charges of conductors are replaced by fictitious charges placed inside the conductor, when this procedure is applied to n contour points, this leads to a linear system of n equations for n unknown charges [11-13].

$$\left[P_{ij} \right]_{n \times n} = \left[Q_j \right]^{-1}_{n} \times V_{ci\ n} \tag{5}$$

Where P_{ij} is the potential coefficients matrix; Q_j is the column vector of fictitious simulation charges; V_{ci} is the column vector of known potentials at the contour point (Boundary conditions).

After determining the values of the simulation charges by solving the matrix system shown in equation 5, it was necessary to check all the calculated charges by choosing new points located on the contour (check points), the new potential V_{vi} is calculated at these check-points, the error tolerance is checked. If this value is lower than the simulation accuracy, the potential and electric field at any point can be calculated, if not, it will be necessary to repeated the all calculations by changing the number and/or the locations of simulation charges [16-19].

4. ELECTRIC FIELD CALCULATION

The conductor of an electrical line is usually represented by an infinite line charges because its length is much greater than the other dimensions, these charges are placed inside the periphery of this conductor. In the charge simulation method (CSM), the effect of the ground is simulated by an image charge for each conductor. This ensures that potential at any point on the ground plane is zero. Using the image technique, each conductor of the line is represented by a positively charged line and a negatively charged image conductor.

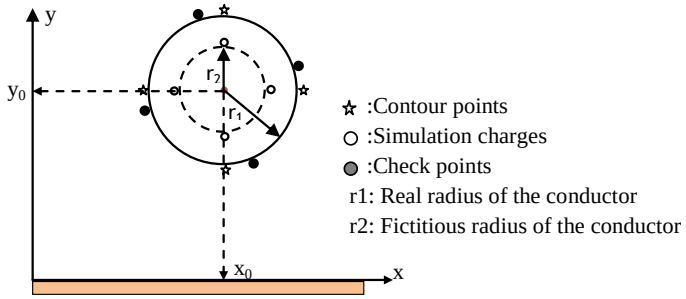

Fig. 2 Arrangement of the simulation charges and the contour points of conductor

The arrangement of fictitious charges and contour points in the conductors of the power line is shown in Fig. 2. The coordinates of these points are calculated using the following formulas [18,21].

$$\begin{aligned} x_k &= x_0 + R \times \cos\left(\frac{2.\pi}{n_k} \times (k-1)\right) \\ y_k &= y_0 + R \times \sin\left(\frac{2.\pi}{n_k} \times (k-1)\right) \end{aligned} \tag{6}$$

Where R= {r_1 if $k=i$, r_2 if $k=j$} ; x_0 is the heights of conductors above ground; y_0 is the horizontal coordinates of conductors.

For an infinite length of charge type, the potential coefficient is given in equation below [18,21].

$$p_{ij} = \frac{1}{(2.\pi \times \varepsilon_0)} \times Ln\left[\frac{\sqrt{(x_i - x_j)^2 + (y_i + y_j)^2}}{\sqrt{(x_i - x_j)^2 + (y_i - y_j)^2}}\right] \tag{7}$$

Where (x_i, y_i) are the coordinates of contour points; (x_j, y_j) are the coordinates of simulation charges.

For a cartesian coordinate system, the magnitude of the total electric field at the desired point is calculated by the summation of the components.

$$E_t = \sqrt{\left(\sum_{j=1}^{n} f_{xi} \times Q_j\right)^2 + \left(\sum_{j=1}^{n} f_{yi} \times Q_j\right)^2} \tag{8}$$

Where f_{xi}, f_{yi} are the field intensity coefficients between the contour points and the simulation charges Qj, they are given below.

$$f_{x_i} = \frac{\partial p_{ij}}{\partial x},\ f_{y_i} = \frac{\partial p_{ij}}{\partial y} \tag{9}$$

In this analysis of electric field created by power transmission line, the catenary form of the overhead power line conductors (conductor sag) is taken into account; this 3D quasi-static analysis can supply to good electric field estimation.

It should be noted that in this analysis, the influence of the towers and metallic objects encountered which act as screens is neglected.

5. SIMPLEX SIMULATED ANNEALING (SIMPSA)

The Simplex Simulated Annealing (SIMPSA) algorithm was developed for the global solution of optimization problems. It is based on the original SA that was proposed for discrete optimization problems. SIMPSA combines the original simulated annealing algorithm (Metropolis algorithm) with the non-linear simplex algorithm (simplex downhill search). Simulated annealing algorithm employs a stochastic generation of solution vectors and employs similarities between the physical process of annealing and a minimization problem. This algorithm shows good robustness and accuracy in arriving at the global optimum of difficult non-convex highly constrained functions [21,22]. Due to the application of the simplex downhill search, a simplex with D + 1 vertex for D decision variable is used. The algorithm starts with an arbitrary solution in the search space, a new solution is created according to the Metropolis algorithm and the fitness function values are calculated for both solutions, the difference between these two points is calculated, the better function evaluation is accepted and becomes the starting point for the next iteration; otherwise a new point is accepted with the Boltzmann probability of $P = \exp(-\Delta E / k_B . T_{\text{int}})$, where ΔE is the difference of fitness function values, k_B is Boltzmann's constant, and T_{init} is the annealing temperature. For the assumed acceptance ratio A_r, the initial annealing temperature T_{init} is estimated by [26-28].

$$A_r = \frac{m_1 + m_2 . e^{-\Delta . E^* / T_{\text{int}}}}{m_1 + m_2} \tag{10}$$

Where m_1 and m_2 are the number of successful and unsuccessful reflections, respectively, ΔE^* is the average increase in objective function values for m_2. In the preliminary generations, the temperature value is remains high, but it is decreased during next generations in order to reduce the acceptance probability. The cooling schedule will then continue with estimated T_{init} by equation (10) as [26-28].

$$T(g+1) = \frac{T(g)}{1 + \frac{T(g) \times \ln(1 + r_{cool})}{3.\sigma}} \tag{11}$$

Where r_{cool} is the cooling rate and σ is the standard deviation of all solutions at *T(g)* (current temperature).

The abovementioned steps are repeated, and the process is continued with a sufficient number of successful generations for the current temperature. The temperature is then gradually reduced using equation (11) and the entire process is repeated until the stopping criterion is met [26-28].

The fitness function used for optimization is based on the accuracy of the calculation method, which is obtained by evaluating the relative error between the potential calculated by the check contour charges and the real potential applied on active conductors. The fitness function (FF) has the form

$$FF = \frac{1}{n_c} \times \sum_{i=1}^{n_c} \left| \frac{V_{c_i} - V_{v_i}}{V_{c_i}} \right| .100 \tag{12}$$

Where V_{ci} is the exact potential to which is subjected the conductors and V_{vi} is the actual voltage of the check charges; n_c is the total number of check points.

The main steps of the proposed GA–CSM algorithm are given as follows [26-28].

1 – SIMPSA generates initial solution with high temperature.
2 – At each step, a new solution is created; the CSM will evaluate the objective function values for both points.
3 – Compare the two solutions using the Metropolis criterion.
4 – Steps 2 and 3 are repeated until system reaches equilibrium state.
5 – Decrease temperature and repeat the above steps, until the stopping criteria are met.

6. FINITE ELEMENT METHOD (FEM)

The finite element method (FEM) is a numerical technique, used to find approximate solutions of partial differential equations, reducing the latter to a system of algebraic equations. The great advantage of this computational technique consists in the fact that the implementation in a code of iterative algorithms, relatively simple, allows having solutions, practically exact, with an acceptable approximation, of very complex problems, with calculation time considerably reduced. The finite element analysis of any problem involves basically four steps. Those are: (a) discrediting the solution region into a finite number of sub-regions or elements, (b) deriving governing equations for a typical element, (c) assembling of all elements in the solution region, and (d) solving the system of equations obtained [29,30]. In bi-dimensional (2D) problems, the energy in an electrostatic field in Cartesian coordinates (*x, y*) has the functional expression [30,31].

$$W_e = \int_S \frac{1}{2} \varepsilon \times E^2 .\, dS = \int_S \frac{1}{2} \varepsilon \times \left\{ \left(\frac{\delta V}{\delta x} \right)^2 + \left(\frac{\delta V}{\delta y} \right)^2 \right\} .\, dS \tag{13}$$

In FEM, the volume of the proposed region is divided into "*m*" small triangular elements where their sides form a grid with "*Ne*" nodes. The potential function is approximated by [31,32].

$$V(r) = \sum_{i=1}^{\mathrm{Ne}} V_i \times f_i(r) \tag{14}$$

Where *Vi* is the electric potential of node *i*, *r* is any point on the proposed region, *fi(r)* represents the shape function having the feature that any *fi(r)* is equal to unit at the location of node *i* and zero at the other nodes.

$$f(r) = (1 \text{ for } i = j), (0 \text{ for } i \neq j) \tag{15}$$

Substituting equation (15) into equation (14), it is obtained the approximate energy *W*, which is minimized under the following conditions.

$$\frac{\delta W_e}{\delta V_i} = 0 \qquad i = 1, 2 \ldots\ldots n \tag{16}$$

A system of equations whose unknowns are the electric potential values in the nodes of the mesh is obtained. The electric field intensity within each element is obtained using the gradient expression as follows.

$$E_i = (-\nabla . V)_m = \sum_{i=1}^{\mathrm{Ne}} V_i \times f_i^m \tag{17}$$

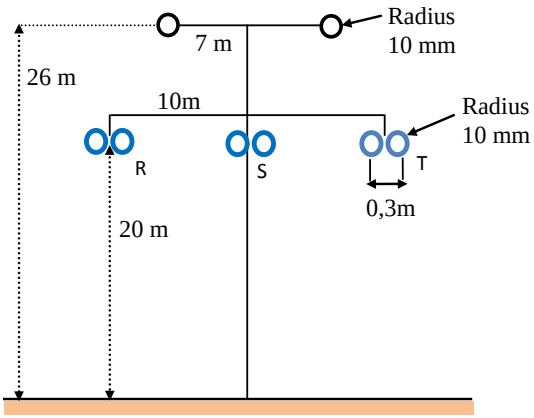

Fig. 3 275 kV Single circuit three phase overhead transmission line

In the present work, a three-phase EHV overhead electrical line of 275 kV with earth wires is considered, with the arrangement and the geometric coordinates, referred to the suspension pylon (height at tower), as shown in Fig. 3, each phase of the transmission line consists of a bundle of two conductors separated by 30 cm with a radius of 10 mm, the ground wire radius is selected as 10 mm, the span length is 300 m, the sag of the conductors s=8 m, and s=6 m for the ground wires. The system of phase voltages is considered

symmetrical and of direct (positive) succession with a nominal frequency of 50 Hz, the earth is assumed to be homogeneous with a resistivity of 100Ω.m.

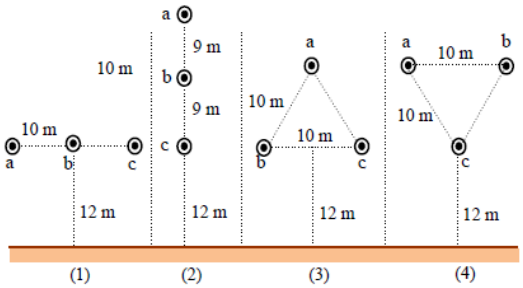

Fig. 4 Different configurations of single circuit lines -
(1) Horizontal, (2) Vertical (3) Triangular, (4) Inverted triangular

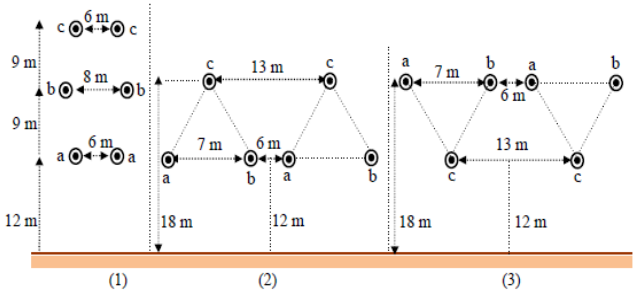

Fig. 5 Different configurations of double circuit lines -
(1) Vertical, (2) Triangular (3) Inverted triangular

6. Results and Discussions

After choosing the type of fictitious charges as infinite line type, the Simplex Simulated Annealing algorithm (SIMPSA) is used to find an appropriate arrangement (number and location) of both fictitious charges and contour points of charge simulation method (CSM) for accurate calculation of electric field. The preferred parameters settings for SIMPSA algorithm taken from [33-35] and search intervals of the variables for the charge simulation method (CSM) are summarized in Table 1.

Table 1 Charge Simulation Method and Simplex Simulated Annealing Parameters

Algorithm+CSM	Number of max generation (iteration) =80
SIMPSA	Cool_rate=10,Min_cooling_factor=0.9,Initial_acceptance_ratio=0.95
CSM	Range of fictitious charges= 4–30. Range of fictitious radius for phase conductor =0.01–0.05 Range of fictitious radius for ground wire =0.001–0.009

After multiple runs for the optimization of the fitness function, once the algorithm terminates execution, the best fitness function value and the optimal parameter values are obtained. The optimal values converged by this algorithm, which are incorporated into the proposed method, are summarized in Table 2:

Table 2 Optimum values of CSM

	Fictitious charges number	Fictitious conductor radius [m]	FF value
Phase conductor	12	0.016	3.64e-12
Ground wire	30	0.0045	

The convergence of the fitness function (FF) mentioned above in equation (12) with number of iterations is shown in Fig. 6. The best value for the fitness function is (3.64e-12) and is practically achieved approximately after 75 iterations.

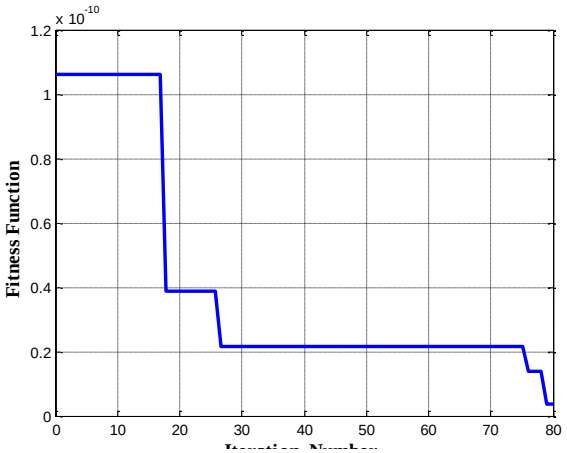

Fig. 6 Convergence of fitness function used in SIMPSA algorithm

The search process of this algorithm at successive iterations with optimal solutions are represented in Figs. 7 and 8 respectively, where it becomes clear that the algorithm converge quickly to these values.

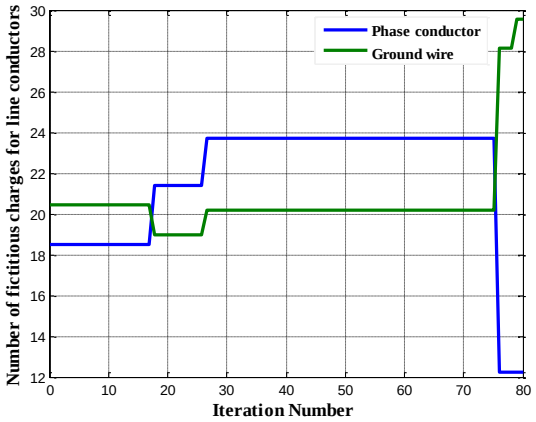

Fig. 7 Convergence of the optimum values of fictitious charges number on the conductor

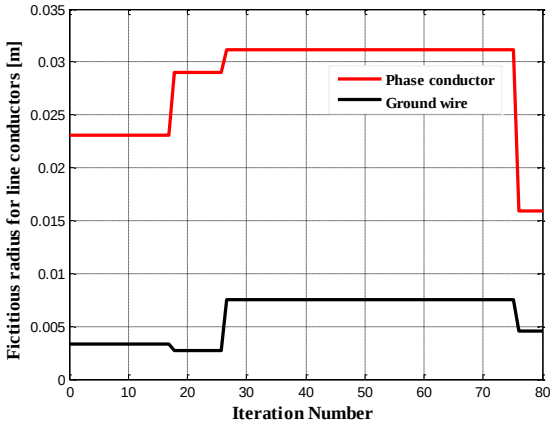

Fig. 8 Convergence of the optimum value of fictitious conductor radius

Fig. 9 shows the lateral profile of the electric field calculated at 1 m above ground level at mid-span length and pylon foot in different points within the right of way. Generally, it is observed that this intensity has a lower value in the centre of the power line, and then increases to a maximum value near under the lateral conductor, from this point; it decreases gradually as the lateral distance from the power line center increases. It appears clear from this figure that the electric field profile is symmetric around the middle conductor.

The most important result which the electric field strength at the mid-span length is significantly higher to that at the pylon (points of suspension), this is due to the effect of the height difference of the conductors above ground level. Consequently, since the suspension height of the conductors above the ground is minimal, the value of the electric field is very high.

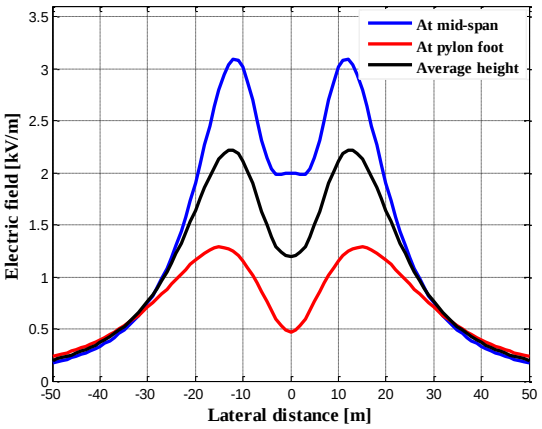

Fig. 9 Electric field profile at mid-span and pylon foot calculated at 1m above the ground

For the average height, the maximum calculated electric field value represents the average value between the maximum value obtained at mid-span and that at the pylon foot. This assumption does not reflect the actual situation of the power line.

The longitudinal profile of the electric field at 1 m above the ground level shown in Fig.10 illustrates very well this observation, the electric field is greatest at mid-span (3.09 kV/m), as the location of the electric field profile approaches the pylon in both directions, the electric field gradually decreases to a minimum value (1.28 kV/m), the electric field near the pylon is much lower than at mid-span.

For the average height, the electric field strength at 1 m above ground level is 2.2 kV/m; this value remains constant along the span of the power line.

This shows that the use of the conductor sagging in the electric field calculation is a very practical way of modeling the real shape of the power line; it plays a considerable role in the determination of the real values of the electric field.

It should be noted that the maximum peak values of the electric field obtained are well below the limits prescribed by the ICNIRP and IRPA international standards.

Fig.11 shows the three-dimensional profile of the electric field over a right of way equal to 50 m either side of the power line center and a span length between the suspension pylons of 300 meters. The values of the higher electric fields exist only in a small area near the mid-span, and then decrease rapidly towards the pylons and even more rapidly away from the side conductors.

Fig.12 describes the mapping of the electric field intensity, in an area defined by the height of the conductors, and the axis of the lateral distance along the corridor. It may be interesting to note that the concentrated level of the electric field is produced around the phase of the conductor surface; the electric field gradually decreases with the lateral distance from the power line center in both directions of the corridor.

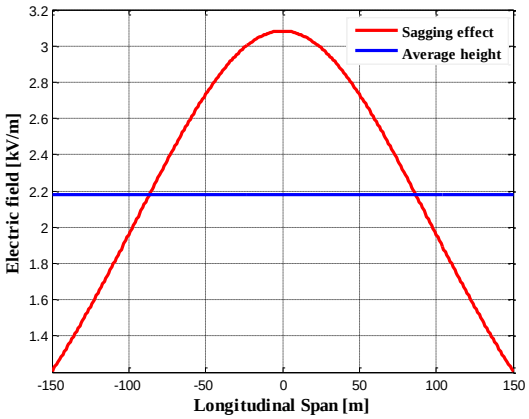

Fig. 10 Longitudinal electric field profile calculated at 1m above the ground

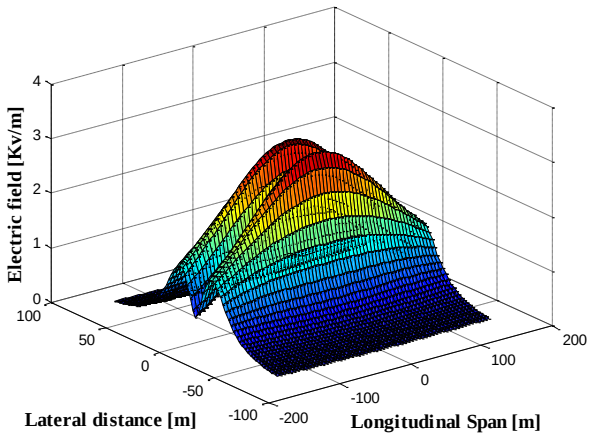

Fig. 11 Three-dimensional (3D) electric field profile calculated at 1 m above the ground

In the following, it should be mentioned some factors which may influence the value of the electric field. The effect of varying the conductor's height and the phase spacing is shown in Fig.13. An increase in the conductor height above the ground (clearance between conductor and ground) causes a significant reduction in the electric field value. An increase of the spacing between phases provokes a slight increase in the strength of the electric field.

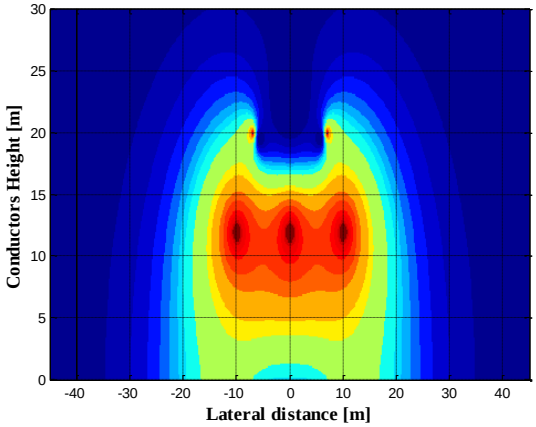

Fig. 12 Mapping of the electric field generated by the single-circuit 275 kV power line at mid-span length

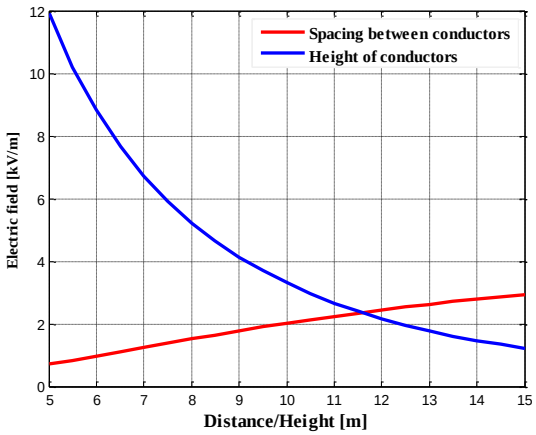

Fig. 13 Electric field profile calculated at 1m above the ground as a function of the conductor height and the spacing between the conductors

Fig.14 illustrates the effect of changing the observation point height of electric field calculation above ground, so it can be seen that the increasing in the calculation point height above ground level can lead as a first step to a small increase in the electric field up to a certain height of 8 m, from this height, the rise becomes sudden. It can be concluded that the amplitude of the electric field is the highest in the immediate vicinity of the surface of the phase conductors and gradually decreases as it goes towards the ground.

Fig.15 shows the effect of bundle phase conductors on the value of the electric field, as seen in this figure, the electric field intensity is slowly increased if the numbers of sub-conductors per phase are increased.

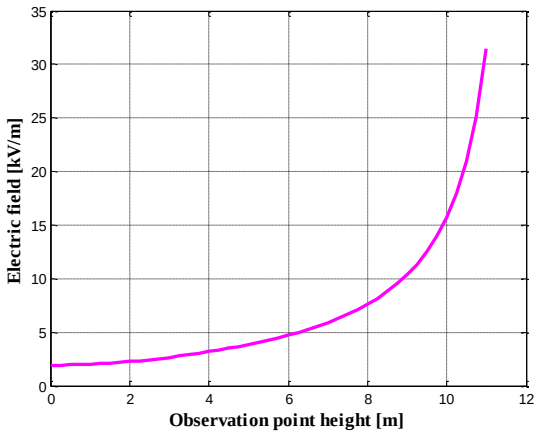

Fig. 14 Electric field profile as a function of the observation point height above ground

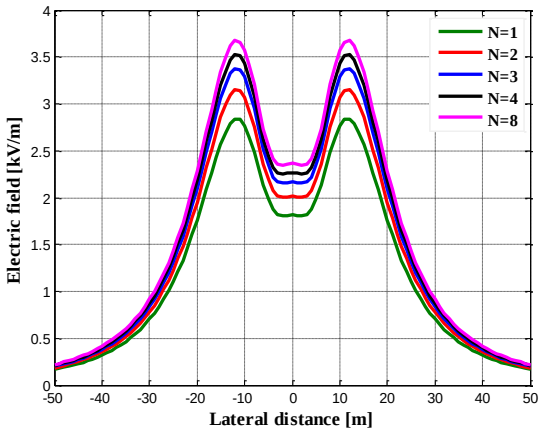

Fig. 15 Electric field profile as a function of the bundle conductors

Electric field profile for different single circuit phase configurations (see Fig.4) is shown in Fig. 16. It can be seen that the horizontal configuration produces the higher maximum electric field than other all configurations due to all conductors being close to the ground level, and on the other hand, the triangular configuration produces the lowest maximum electric field due to better cancellation effect of the line voltages.

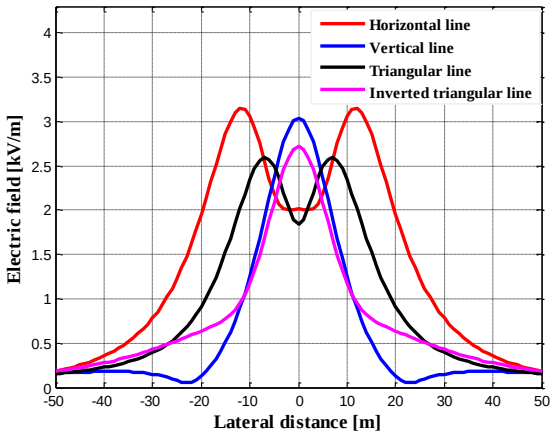

Fig. 16 Lateral electric field profile calculated at 1m above the ground for different phase configurations of single-circuit 275 kV transmission line

For various double circuit configurations lines (see Fig. 5), for the same phasing (abc-abc), the lateral distribution of electric field is illustrated by Fig.17. Typically, one can observe that the triangular configuration gives lower maximum electric field than the other configurations in the immediate vicinity of the power line center into an interval between [-7,+7] m, for a distance between 7 and 30 m ±[7-30], the vertical configuration is the preferred configuration, within this range the values obtained indicate a significant reduction in the electric field strength.

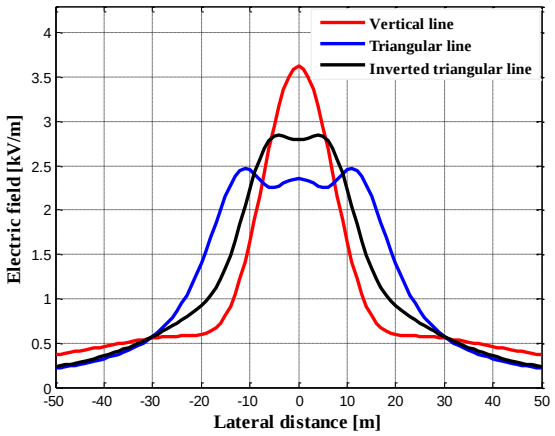

Fig. 17 Lateral electric field profile calculated at 1 m above the ground for different phase configurations of double-circuit 275 kV transmission line

In double circuit overhead power line, the phase sequence arrangement has a significant influence on the electric field intensity; it is highly possible to adjust the position of the phase order to reduce the electric field under the power line to a lower level. As an example, the electric field for different phase arrangements in a vertical double circuit line with the same parameters is illustrated in Fig. 18. As can be seen in this figure, the inverse phase arrangement (abc-cba) or low-reactance phasing gives the lowest value of electric field for the different points along the power line corridor, because of the best electric field cancellation caused by the phase- shift between phases, while the phase arrangement (abc-acb) produces a higher electric field than all other arrangements of phase conductors.

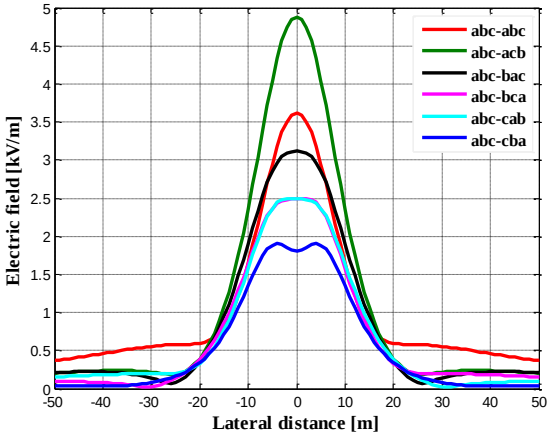

Fig. 18 Comparison of electric field in different phase's arrangement for double circuit vertical line 275 kV

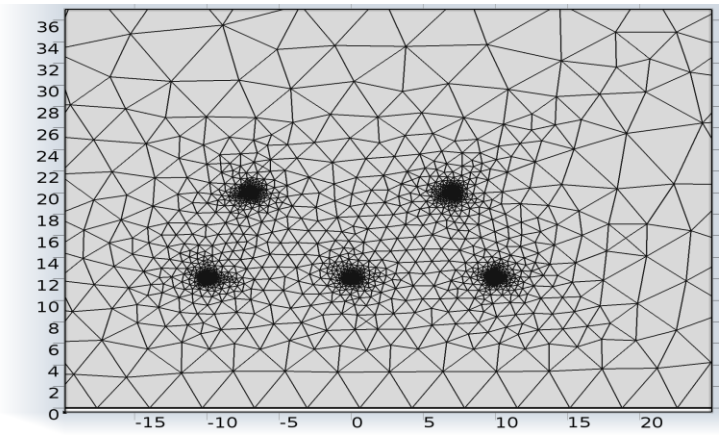

Fig. 19 Finite element discretization of the study domain given in Fig. 3

In order to validate the adopted method in this study, the COMSOL Multiphysics software (version 4.3b) specializing in electromagnetism numerical simulation based on the finite element method (FEM) can be used to simulate and evaluate the electric field around the overhead power lines.

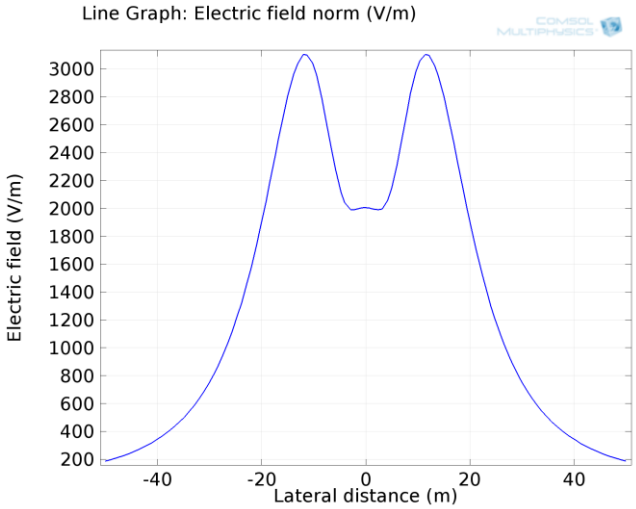

Fig. 20 Electric field profile at mid-span length calculated at 1m above the ground using COMSOL 4.3b software

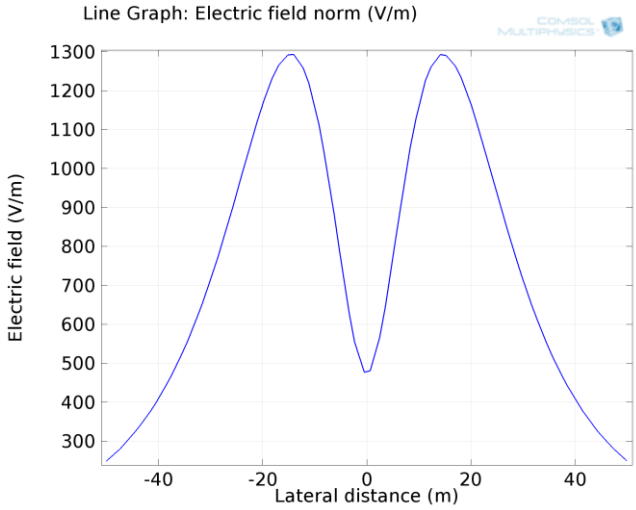

Fig. 21 Electric field profile at pylon foot calculated at 1m above the ground using COMSOL 4.3b software

The electrostatic module was appropriately chosen for this computational work to solve and analyze this model in 2D dimensional space. The Mesh using linear triangular elements generated by this software in the study domain with the defined settings of the system is shown in Fig. 19.

Figs. 20 and 21 respectively, show the electric field distribution at mid-span length and pylon foot under the HV power line at 1 m above the ground level using the COMSOL 4.3b software.

It can be seen that the electric field under the middle conductor is less intense, and then it increases to a maximum intensity nearly under the lateral conductors. As the distance from this point increases, the electric field strength decreased quite rapidly.

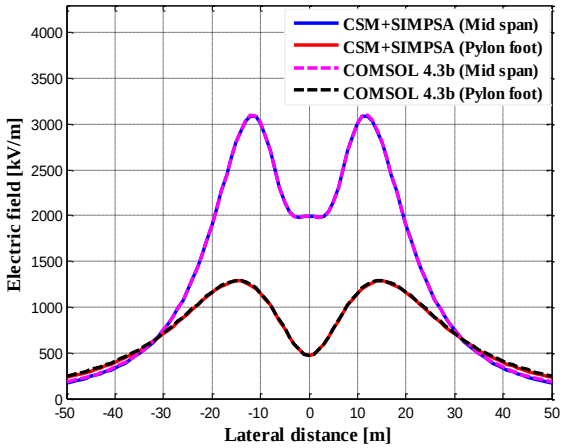

Fig. 22 Comparison of Electric field levels between the proposed method and COMSOL 4.3b software

The comparison of the electric field results obtained by the proposed method with those simulated from COMSOL 4.3b software is shown in Fig. 22. These results are in good agreement; the graphs of two figures are approximately superposed, the maximum error value is not significant; it does not exceed the value of 4.8%.

7. CONCLUSION

In this study, a novel optimized approach that couples the Simplex Simulated Annealing algorithm (SIMPSA) and the charge simulation method (CSM) has been presented. The adopted algorithm offers efficiency and accuracy for determination of the optimal position and number of fictitious charges. Accurate results on the 3D quasi-static analysis of electric field created by an EHV overhead power line have been obtained. From the results, it is clear that the electric field intensity is less intense under the middle phase conductor and increases to peak intensity near under the side phase conductor; then decreases with increasing the lateral distance. It has also been found that the electric field depends on several factors, such as the spacing between two adjacent conductors and conductor height above the ground, the type of

lines, single or double circuit. For double circuit lines, it is possible to adjust the phases in an appropriate manner in order to achieve a significant reduction of the electric field.

The most important parameter is the influence of the conductor sag; it is noted that the value of the electric field at mid-span length is much higher than that at the pylon foot. The obtained results were compared with those obtained from the COMSOL 4.3b software. The simulation results are almost identical and are visually superimposed; the comparison is satisfying enough and it sufficient to validate the combined method.

REFERENCES

[1] Ch. J. Portier, M.S. Wolfe, "Assessment of Health Effects from Exposure to Power-Line Frequency Electric and Magnetic Fields," Working Group Report, NIEHS and EMFRAPID, August 1998.

[2] The ELF Working Group, health effects and exposure guidelines related to extremely low frequency electric and magnetic fields, The Federal Provincial Territorial Radiation Protection Committee, Canada, January 2005.

[3] T. Keikko, "Technical Management of the Electric and Magnetic Fields in Electric Power System," Technical Report, Finland, 2003.

[4] CIGRE, "Electric and magnetic fields produced by transmission systems," Description of phenomena-Practical Guide for calculation, WG 36-01, Paris 1980.

[5] Report, "A Review of the Potential Health Risks of Radiofrequency Fields from Wireless Telecommunication Devices," the Royal Society of Canada, RSC.EPR 99-1, March 1999.

[6] ICNIRP, " International Commission on Non-Ionizing Radiation Protection, "Guidelines for limiting exposure to time-varying electric and magnetic fields (1Hz to 100 kHz)," *Health Physics*, vol. 99, no.6, pp. 818–836, 2010.

[7] IARC, "Non-ionizing radiation, Part 1: Static and extremely low-frequency (ELF) electric and magnetic fields," IARC Monographs on the Evaluation of Carcinogenic Risks to Humans," vol. 80, pp.1-395, 2002.

[8] WHO, "Extremely low frequency fields, Environmental Health Criteria Monograph, " no. 238, WHO Press, Geneva, Switzerland, 2007.

[9] Abstract Book, "International Conference on Electromagnetic Fields, Bio-effects to Legislation", Ljubljana, Slovenia, November 2004.

[10] Review , Statement of the International Evaluation Committee to Investigate the Health Risks of Exposure to Electric, Magnetic and Electromagnetic Fields, The Italian Ministers of Environment, Health and Telecommunication, Italy,2002.

[11] H. Singer, H. Steinhigler, P. Weiss, "A charge simulation methods for the calculation of high voltage fields," *IEEE Trans on Power Applicat*, vol. PAS-93, pp. 3660-3668, 1974.

[12] T. Takuma, "charge simulation method with complex fictitious charges for calculating capacitive resistive fields," *IEEE Trans on Power Apparatus and Systems*, vol. PAS-I00, no.11, pp. 4665-4672, November 1981.

[13] N.H. Malik, "A Review of the Charge Simulation Method and its Applications," *IEEE Trans on Electrical Insulation*, vol. 24, no.1, pp.3-20, Feb 1989.

[14] S. Chakravorti, P. K. Mukherjee, "Efficient field calculation in three-core belted cable by charge simulation using complex charges," *IEEE Trans on Electrical Insulation*, vol. 27, no. 6, pp. 1208-1212, 1992.

[15] X. M. Liu, Y. D Cao, E. Z. Wang, "Numerical Simulation of Electric Field With Open Boundary Using Intelligent Optimum Charge Simulation Method," *IEEE Transactions on Magnetics*, vol. 42, no. 4, pp.1159-1162, April 2006.

[16] D. Himadri, "Implementation of Basic Charge Configurations to Charge Simulation Method for Electric Field Calculations," *International journal of advanced research in electrical, electronics and instrumentation engineering*, vol. 3, no.5, pp. 9607-9611, May 2014.

[17] R. M. Radwn, M. M. Samy , "Calculation of Electric Fields underneath Six Phase Transmission Lines," *Journal of electrical systems*, vol.12, no. 4, pp.839-851, 2016.

[18] R. Djekidel, D. Mahi, "Effect of the shield lines on the electric field intensity around the High Voltage overhead transmission lines," *International Journal of Modeling, Measurement and Control A, AMSE Journals, Series, Modelling A*, vol.87, no. 1, pp. 1-16, 2014.

[19] M. M. Samy, A. M. Emam, "Computation of electric fields around parallel HV and EHV overhead transmission lines in Egyptian power network," In Proceedings of the IEEE, International Conference on

Environment and Electrical Engineering and IEEE Industrial and Commercial Power Systems Europe, Italy, 2017, pp. 1 – 5.

[20] R. Djekidel, A, Choucha, A, Hadjaj, "Efficiency of some optimization approaches with the charge simulation method for calculating the electric field under extra high voltage power lines," *IET Generation, Transmission and Distribution* , vol. 11, no. 17, pp.4167 – 4174, 2017.

[21] M. F. Cardoso, R. L. Salcedo, S. F. de Azevedo, "The simplex-simulated annealing approach to continuous non-linear optimization", *Computers & Chemical Engineering*, vol. 20, no. 9, pp. 1065-1080, Sep 1996.

[22] M. E. Cardoso, R. L. Salcedo, S. F. Azevedo, D. Barbosa, "A simulated annealing approach to the solution of minlp problems", *Computers & Chemical Engineering.*, vol. 21, no. 12, pp. 1349-1364, 1997.

[23] A. V. Mamishev, R. D. Nevels, and B. D. Russell , "Effects of Conductor Sag on Spatial Distribution of Power Line Magnetic Field," *IEEE Trans on Power Delivery*, vol. 11, no. 3, pp. 1571-1576, July 1996.

[24] M.P.Arabani, B.Porkar, S.Porkar, "The influence of conductor sag on spatial distribution of transmission line magnetic field," Cigre, paper B2–202, Paris, 2004.

[25] V. Phan Tu, J. Tlusty," The Induced Magnetic Field Calculation of Three Phase Overhead Transmission Lines Above a Lossy Ground as a Frequency-Dependent Complex Function", In Proceedings of the IEEE Conference on power Engineering, Canada, May 2003, pp. 154 – 158.

[26] R. Mukesh, K. Lingadurai, "Aerodynamic Optimization Using Simulated Annealing and its. Variants", *International Journal of Engineering Trends and Technology*, vol.2, no. 3, pp.73–77, 2011.

[27] H. Ketabchi, B. Ataie-Ashtiani, "Evolutionary algorithms for the optimal management of coastal groundwater: A comparative study toward future challenges," *Journal of Hydrology*, vol. 520, pp.193-213, 2015.

[28] B. Behzadi, C. Ghotbi, A. Galindo, "Application of the simplex simulated annealing technique to nonlinear parameter optimization for the SAFT-VR equation of state," *Chemical Engineering Science,science direct*, vol.60, no. 3 , pp. 6607–6621, Dec 2005.

[29] M. K. Haldar, "Introducing the Finite Element Method in electromagnetics to undergraduates using Matlab," *International Journal of Electrical Engineering Education*, vol. 43, pp. 232-244, 2006.

[30] E. O. Virjoghe, D. E. Nescu, M. F. Stan, C. Cobianu, "Numerical determination of electric field around a high voltage electrical overhead line, " *Journal of Science and Arts*, vol. 4, no. 21, pp. 487-496, 2012.

[31] N.Yadav, N. Kumar, "2-Dimensional and 3-Dimesional Electromagnetic Fields Using Finite element method," *IOSR, Journal of Electrical and Electronics Engineering*, vol. 7, no. 2, pp. 53-60, 2013.

[32] J. Faiz, M. Ojaghi, "Instructive Review of Computation of Electric Fields using Different Numerical Techniques", *International Journal of Engineering*, vol. 18, no. 3, pp. 344-356, 2002.

[33] S. Bera, I. Mukherjee, "An Ellipsoidal Distance-based Search Strategy of Ants for Nonlinear Single and Multiple Response Optimization Problems," *European Journal of Operations Research*, vol. 223, no. 2, pp. 321-332, 2012.

[34] Z.H. Che, H.S. Wang, "A hybrid approach for supplier cluster analysis," *Computers & Mathematics with Applications*, vol. 59, no. 2, pp. 745–763, 2010.

[35] M. M. Atiqullah, "An Efficient Simple Cooling Schedule for Simulated Annealing," In Proceedings of the international Conference on Computational Science and Its Applications, Italy, pp 396-404, May 2004.